

## NiSO<sub>4</sub> Supported on FeO-promoted ZrO<sub>2</sub> Catalyst for Ethylene Dimerization

Jong Rack Sohn,\* Young Tae Kim, and Dong Cheol Shin

Department of Applied Chemistry, Engineering College, Kyungpook National University, Daegu 702-701, Korea

\*E-mail: jrsohn@knu.ac.kr

Received August 3, 2005

The NiSO<sub>4</sub> supported on FeO-promoted ZrO<sub>2</sub> catalysts were prepared by the impregnation method. FeO-promoted ZrO<sub>2</sub> was prepared by the coprecipitation method using a mixed aqueous solution of zirconium oxychloride and iron nitrate solution followed by adding an aqueous ammonia solution. The addition of nickel sulfate (or FeO) to ZrO<sub>2</sub> shifted the phase transition of ZrO<sub>2</sub> (from amorphous to tetragonal) to higher temperatures because of the interaction between nickel sulfate (or FeO) and ZrO<sub>2</sub>. 10-NiSO<sub>4</sub>/5-FeO-ZrO<sub>2</sub> containing 10 wt % NiSO<sub>4</sub> and 5 mol % FeO, and calcined at 500 °C exhibited a maximum catalytic activity for ethylene dimerization. NiSO<sub>4</sub>/FeO-ZrO<sub>2</sub> catalysts were very effective for ethylene dimerization even at room temperature, but FeO-ZrO<sub>2</sub> without NiSO<sub>4</sub> did not exhibit any catalytic activity at all. The catalytic activities were correlated with the acidity of catalysts measured by the ammonia chemisorption method. The addition of FeO up to 5 mol % enhanced the acidity, surface area, thermal property, and catalytic activities of catalysts gradually, due to the interaction between FeO and ZrO<sub>2</sub> and due to consequent formation of Fe-O-Zr bond.

**Key Words :** FeO-promoted NiSO<sub>4</sub> catalyst, Acid strength, Acidity, Ethylene dimerization

### Introduction

Heterogeneous catalysts for the dimerization and oligomerization of olefins, consisting mainly of nickel compounds supported on oxides, have been known for many years. A considerable number of papers have dealt with the problem of nickel-containing catalysts for ethylene dimerization.<sup>1-11</sup> One of the remarkable features of this catalyst system is its activity in relation to a series of *n*-olefins. In contrast to usual acid-type catalysts, nickel oxide on silica or silica-alumina shows a higher activity for a lower olefin dimerization, particularly for ethylene.<sup>1-6,12</sup> It has been suggested that the active site for dimerization is formed by an interaction of a low-valent nickel ion with an acid site.<sup>9,13</sup> In fact, nickel oxide, which is active for C<sub>2</sub>H<sub>4</sub>-C<sub>2</sub>D<sub>4</sub> equilibration, acquires an activity for ethylene dimerization upon addition of nickel sulfate, which is known to be an acid.<sup>14</sup> A transition metal can also be supported on zeolite in the state of a cation or a finely dispersed metal. Transition metal ions like Ni<sup>2+</sup> or Pd<sup>2+</sup> can be active sites in catalytic reactions such as ethylene and propylene dimerization as well as acetylene cyclomerization.<sup>15-17</sup>

The previous papers from this laboratory have shown that NiO-TiO<sub>2</sub> and NiO-ZrO<sub>2</sub> modified with sulfate or tungstate ions are very active for ethylene dimerization.<sup>6,18-20</sup> High catalytic activities in the reactions were attributed to the enhanced acidic properties of the modified catalysts, which originated from the inductive effect of S=O or W=O bonds of the complex formed by the interaction of oxides with sulfate or tungstate ions. However, catalytic functions have been improved by loading additional components. Sulfated zirconia incorporating Fe and Mn has been shown to be highly active for butane isomerization, catalyzing the reaction even at room temperature.<sup>21,22</sup> The promotion in

activity of catalyst has been confirmed by several other research groups.<sup>23-25</sup> Coelho *et al.* have discovered that the addition of Ni to sulfated zirconia causes an activity enhancement comparable to that caused by the addition of Fe and Mn.<sup>26</sup> It has been reported by several workers that the addition of platinum to zirconia modified by sulfate ions enhances catalytic activity in the skeletal isomerization of alkanes without deactivation when the reaction is carried out in the presence of hydrogen.<sup>27-29</sup> Recently, it has been found that a main group element Al can also promote the catalytic activity and stability of sulfated zirconia for *n*-butane isomerization and ethylene dimerization.<sup>30-32</sup>

Many metal sulfates generate fairly large amounts of acid sites of moderate or strong strength on their surfaces when they are calcined at 400-700 °C.<sup>33,34</sup> The acidic property of metal sulfate often gives high selectivity for diversified reactions such as hydration, polymerization, alkylation, cracking, and isomerization. However, structural and physico-chemical properties of supported metal sulfates are considered to be in different states compared with bulk metal sulfates because of their interaction with supports.<sup>9,10,35</sup> Our previous work has shown that NiSO<sub>4</sub> supported on ZrO<sub>2</sub> is active for ethylene dimerization.<sup>36</sup> As an extension of the study on the ethylene dimerization, we prepared a new catalyst of NiSO<sub>4</sub>/FeO-ZrO<sub>2</sub> and the promoting effect of FeO on catalytic activity was studied.

### Experimental Section

**Catalyst preparation.** The FeO-ZrO<sub>2</sub> mixed oxide was prepared by a co-precipitation method using aqueous ammonia as the precipitation reagent. The coprecipitate of Fe(OH)<sub>2</sub>-Zr(OH)<sub>4</sub> was obtained by adding aqueous ammonia slowly into a mixed aqueous solution of iron (II)

chloride and zirconium oxychloride (Junsei Chemical Co.) at room temperature with stirring until the pH of the mother liquor reached about 8. Catalysts containing various nickel sulfate contents were prepared by the impregnation of  $\text{Fe}(\text{OH})_2\text{-Zr}(\text{OH})_4$  powder with an aqueous solution of  $\text{NiSO}_4$ , followed by calcining at different temperatures for 1.5 h in air. This series of catalysts is denoted by the mol percentage of FeO and the weight percentage of nickel sulfate. For example, 10- $\text{NiSO}_4/5\text{-FeO-ZrO}_2$  indicates the catalyst containing 5 mol % of FeO and 10 wt % of  $\text{NiSO}_4$ .

**Procedure.** FTIR spectra were obtained in a heatable gas cell at room temperature using a Mattson Model GL6030E spectrophotometer. The self-supporting catalyst wafers contained about  $10 \text{ mg cm}^{-2}$ . Prior to obtaining the spectra, we heated each sample under vacuum at 25-500 °C for 1 h. Catalysts were checked in order to determine the structure of the prepared catalysts by means of a Philips X'pert-APD X-ray diffractometer, employing Ni-filtered Cu  $K_\alpha$  radiation. DSC measurements were performed by a PL-STA model 1500H apparatus in air; the heating rate was 5 °C per minute. For each experiment 10-15 mg of sample was used.

The specific surface area was determined by applying the BET method to the adsorption of  $\text{N}_2$  at  $-196$  °C. Chemisorption of ammonia was also employed as a measure of the acidity of catalysts. The amount of chemisorption was determined based on the irreversible adsorption of ammonia.<sup>20,37,38</sup>

The catalytic activity for ethylene dimerization was determined at 20 °C using a conventional static system following the pressure change from an initial pressure of 290 Torr. A fresh catalyst sample of 0.2 g was used for every run and the catalytic activity was calculated as the initial rate calculated from the initial activity slope. Reaction products were analyzed by gas chromatography with a VZ-7 column at room temperature.

## Results and Discussion

**Infrared Spectra.** The infrared spectra of 10- $\text{NiSO}_4/5\text{-FeO-ZrO}_2$  (KBr disc) calcined at different temperatures (400-800 °C) are given in Figure 1. 10- $\text{NiSO}_4/5\text{-FeO-ZrO}_2$  calcined up to 700 °C showed infrared absorption bands at 1206, 1134, 1064 and 989  $\text{cm}^{-1}$ , which are assigned to bidentate sulfate ions coordinated to the metal such as  $\text{Zr}^{4+}$  or  $\text{Fe}^{2+}$ .<sup>39,40</sup> The band at 1625  $\text{cm}^{-1}$  is assigned to the deformation vibration mode of the adsorbed water. For 10- $\text{NiSO}_4/5\text{-FeO-ZrO}_2$  calcined at 700 °C, the band intensities of sulfate ion decreased because of the partial decomposition of sulfate ion. However, for the sample calcined at 800 °C, infrared bands by the sulfate ion disappeared completely due to the decomposition of sulfate ion.

In general, for the metal oxides modified with sulfate ions followed by evacuation above 400 °C, a strong band<sup>41,42</sup> assigned to S=O stretching frequency is observed at 1390-1360  $\text{cm}^{-1}$ . In a separate experiment, the infrared spectrum of self-supported 10- $\text{NiSO}_4/5\text{-FeO-ZrO}_2$  after evacuation at 25-500 °C for 1 h was examined. As shown in Figure 2, an intense band at 1342-1370  $\text{cm}^{-1}$  accompanied by four broad

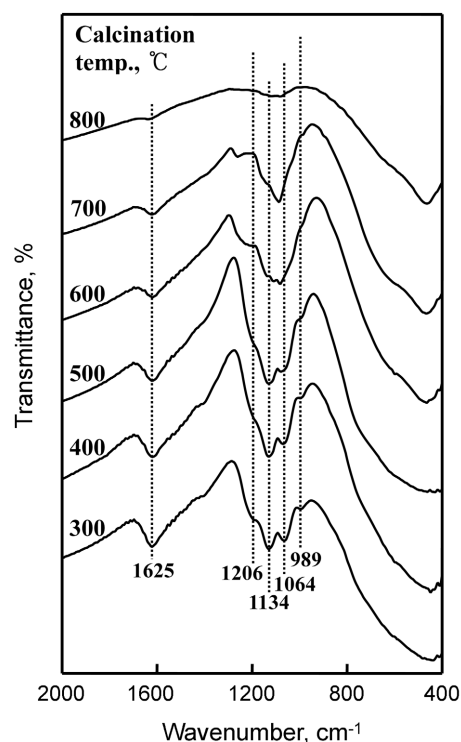


**Figure 1.** Infrared spectra of 10- $\text{NiSO}_4/5\text{-FeO-ZrO}_2$  calcined at different temperatures for 1.5 h.

but split bands at 1201, 1130, 1060 and 1012  $\text{cm}^{-1}$ , indicating the presence of different adsorbed species depending on the treatment conditions of the sulfated sample.<sup>43</sup> At 25 °C an asymmetric stretching band of S=O bonds was not observed because water molecules are adsorbed on the surface of 15- $\text{NiSO}_4/5\text{-FeO-ZrO}_2$ .<sup>30,44</sup> At 100 °C the S=O stretching band appeared at 1342  $\text{cm}^{-1}$ . The band intensity increased with the evacuation temperature and the position of band shifted to a higher wavenumber. That is, the higher the evacuation temperature, the larger was the shift of the asymmetric stretching frequency of the S=O bonds. It is likely that the surface sulfur complexes formed by the interaction of oxides with sulfate ions in highly active catalysts have a strong tendency to reduce their bond order by the adsorption of basic molecules such as  $\text{H}_2\text{O}$ .<sup>30,44</sup> When the 15- $\text{NiSO}_4/5\text{-FeO-ZrO}_2$  sample evacuated at 500 °C was exposed to air at 25 °C, the drastic shift of the IR band from 1370  $\text{cm}^{-1}$  to lower wavenumber (not shown due to the overlaps with skeletal vibration band of FeO and  $\text{ZrO}_2$ ) occurred because of the adsorption of water, resulting in the appearance of adsorbed water band at 1625  $\text{cm}^{-1}$ . Consequently, as shown in Figure 2, an asymmetric stretching band of S=O bonds for the sample evacuated at a lower temperature appears at a lower frequency compared with that for the sample evacuated at higher temperature, because the adsorbed water reduces the bond order of S=O from a highly covalent double-bond character to a lesser double-bond character.

**Crystalline Structures of Catalysts.** The crystalline structures of catalysts calcined in air at different temper-

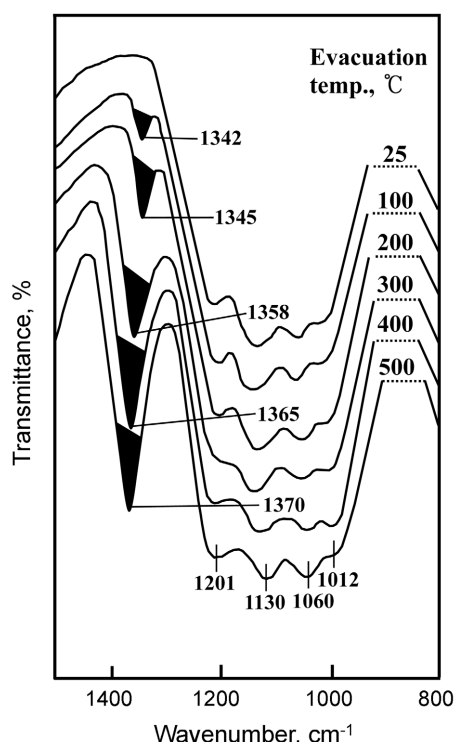


**Figure 2.** Infrared spectra of 10-NiSO<sub>4</sub>/5-FeO-ZrO<sub>2</sub> evacuated at different temperatures for 1 h.

atures for 1.5 h were examined. In the case of zirconia support, ZrO<sub>2</sub> was amorphous to XRD up to 300 °C, with tetragonal phase at 350 °C, a two-phase mixture of the tetragonal and monoclinic forms at 400-800 °C, and a

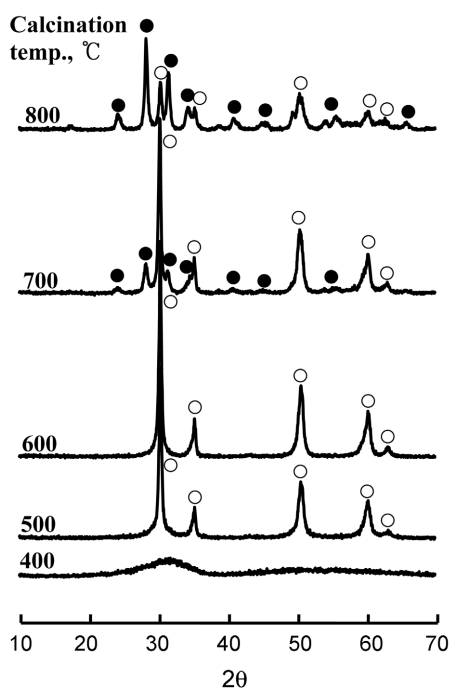


**Figure 3.** X-ray diffraction patterns of 5-FeO-ZrO<sub>2</sub> calcined at different temperatures for 1.5 h: (○), tetragonal phase of ZrO<sub>2</sub>; (●), monoclinic phase of ZrO<sub>2</sub>.

monoclinic phase at 900 °C (This figure is not shown here.) Three crystal structures of ZrO<sub>2</sub>, *i.e.*, tetragonal, monoclinic, and cubic phase have been reported.<sup>32,37</sup>

However, as shown in Figure 3, in the case of 5-FeO-ZrO<sub>2</sub>, the crystalline structures of the samples were different from the structure of pure ZrO<sub>2</sub>. 5-FeO-ZrO<sub>2</sub> calcined at 400 °C are amorphous. The transition temperature of ZrO<sub>2</sub> from amorphous to tetragonal phase was higher by 100 °C than that of pure ZrO<sub>2</sub>. X-ray diffraction data indicated the tetragonal phase of ZrO<sub>2</sub> at 500-600 °C, and a two-phase mixture of the tetragonal and monoclinic ZrO<sub>2</sub> forms at 700-800 °C. It is assumed that the interaction between FeO and ZrO<sub>2</sub> hinders the phase transition of ZrO<sub>2</sub> from amorphous to tetragonal, and from tetragonal to monoclinic.<sup>30,32,37</sup>

The crystalline structures of 10-NiSO<sub>4</sub>/5-FeO-ZrO<sub>2</sub> calcined in air at different temperatures for 1.5 h were checked by X-ray diffraction. In the case of supported nickel sulfate catalysts, the crystalline structures of the samples were also different from the structure of the ZrO<sub>2</sub> support. The 10-NiSO<sub>4</sub>/5-FeO-ZrO<sub>2</sub> materials calcined at different temperatures, as shown in Figure 4, are amorphous up to 500 °C. In other words, the transition temperature from amorphous to tetragonal phase was higher by 250 °C than that of pure ZrO<sub>2</sub>.<sup>36</sup> X-ray diffraction data indicated only the tetragonal phase of ZrO<sub>2</sub> at 600-800 °C, without detection of orthorhombic NiSO<sub>4</sub> phase. It is assumed that the interaction between NiSO<sub>4</sub> (or FeO) and ZrO<sub>2</sub> hinders the phase transition of ZrO<sub>2</sub> from amorphous to tetragonal.<sup>30</sup> For the above FeO-promoted catalysts, there are no characteristic peaks of FeO in the patterns, implying that FeO is sufficiently homogeneously mixed with zirconia and that

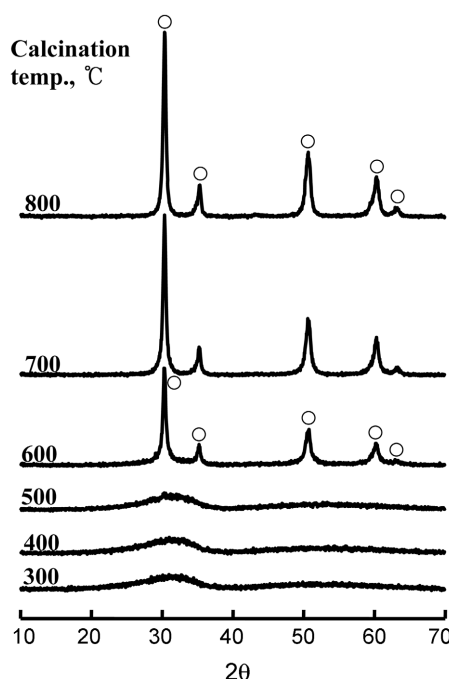


**Figure 4.** X-ray diffraction patterns of 10-NiSO<sub>4</sub>/5-FeO-ZrO<sub>2</sub> calcined at different temperatures for 1.5 h: (○), tetragonal phase of ZrO<sub>2</sub>.

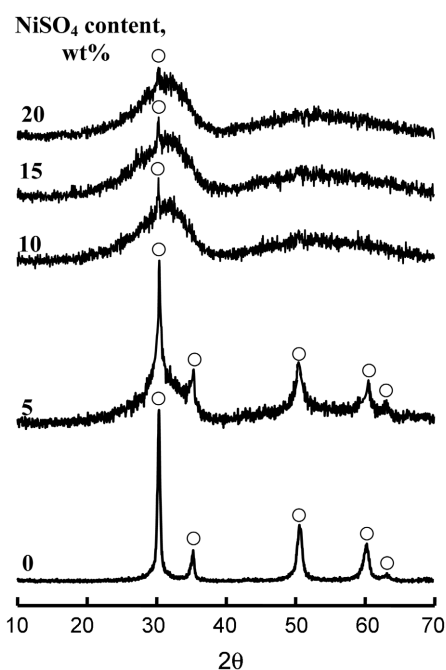


**Figure 5.** X-ray diffraction patterns of NiSO<sub>4</sub>/5-FeO-ZrO<sub>2</sub> containing different NiSO<sub>4</sub> contents and calcined at 500 °C for 1.5 h: (○), tetragonal phase of ZrO<sub>2</sub>.

FeO is well dispersed on the surface of ZrO<sub>2</sub>. Also, there is a possibility that some of FeO is oxidized during calcination and that consequently Fe<sub>3</sub>O<sub>4</sub> coexists with FeO.

The XRD patterns of NiSO<sub>4</sub>/5-FeO-ZrO<sub>2</sub> containing different nickel sulfate contents and calcined at 500 °C for 1.5 h are shown in Figure 5. XRD data indicated mostly amorphous phase of ZrO<sub>2</sub> together with tiny amount of tetragonal ZrO<sub>2</sub> phase at the region of 10–20 wt % of nickel sulfate, indicating good dispersion of NiSO<sub>4</sub> on the surface of 5-FeO-ZrO<sub>2</sub>. However, for 5-NiSO<sub>4</sub>/5-FeO-ZrO<sub>2</sub> containing small amount of NiSO<sub>4</sub> (5 wt%), XRD data showed only tetragonal phase of ZrO<sub>2</sub> due to the less interaction between NiSO<sub>4</sub> and ZrO<sub>2</sub>. Moreover, for 5-FeO-ZrO<sub>2</sub> sample without NiSO<sub>4</sub>, only high crystalline of tetragonal ZrO<sub>2</sub> phase was observed because of the easiness of ZrO<sub>2</sub> phase transition from amorphous to tetragonal due to no interaction between NiSO<sub>4</sub> and ZrO<sub>2</sub>.

The XRD patterns of 10-NiSO<sub>4</sub>/FeO-ZrO<sub>2</sub> containing different FeO contents and calcined at 500 °C for 1.5 h are shown in Figure 6. XRD data indicated only tiny amount of tetragonal ZrO<sub>2</sub> phase at the region of 3–10 mol % of FeO. However, the higher the content of FeO, the lower is the amount of tetragonal ZrO<sub>2</sub> phase as in the case of NiSO<sub>4</sub> addition, showing only amorphous phase for the sample above 5 mol % FeO, because the interaction between FeO and ZrO<sub>2</sub> hinders the phase transition of ZrO<sub>2</sub> from amorphous to tetragonal in proportion to the FeO content.<sup>40</sup> In this case, no crystalline phase of FeO was observed on the X-ray diffraction patterns.

**Thermal Analysis.** The X-ray diffraction patterns in Figures 3–6 clearly show that the structure of NiSO<sub>4</sub>/FeO-ZrO<sub>2</sub> is different depending on the calcined temperature. To

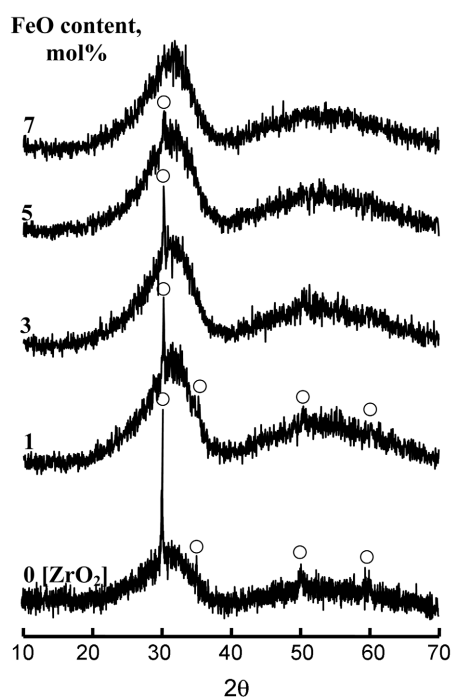


**Figure 6.** X-ray diffraction patterns of 10-NiSO<sub>4</sub>/FeO-ZrO<sub>2</sub> containing different FeO contents and calcined at 500 °C for 1.5 h: (○), tetragonal phase of ZrO<sub>2</sub>.

examine the thermal properties of precursors of NiSO<sub>4</sub>/FeO-ZrO<sub>2</sub> samples more clearly, we completed their thermal analysis; the results are illustrated in Figures 7 and 8. For pure ZrO<sub>2</sub>, the DSC curve shows a broad endothermic peak below 200 °C due to water elimination, and a sharp exothermic peak at 427 °C due to the ZrO<sub>2</sub> crystallization.<sup>40</sup> However, it is of interest to see the influence of FeO on the crystallization of ZrO<sub>2</sub> from amorphous to tetragonal phase. As Figure 7 shows, the exothermic peak due to the crystallization appears at 427 °C for pure ZrO<sub>2</sub>, while for FeO-ZrO<sub>2</sub> samples it is shifted to higher temperatures due to the interaction between FeO and ZrO<sub>2</sub>. The shift increases with increasing FeO content. Consequently, the exothermic peaks appear at 439 °C for 1-FeO-ZrO<sub>2</sub>, 444 °C for 3-FeO-ZrO<sub>2</sub>, 447 °C for 5-FeO-ZrO<sub>2</sub>, 455 °C for 7-FeO-ZrO<sub>2</sub>, and 474 °C for 10-FeO-ZrO<sub>2</sub>.

However, for NiSO<sub>4</sub>/5-FeO-ZrO<sub>2</sub> samples containing different NiSO<sub>4</sub> contents, the DSC patterns are somewhat different from that of FeO-ZrO<sub>2</sub>. As shown in Figure 8, the exothermic peak for NiSO<sub>4</sub>/5-FeO-ZrO<sub>2</sub> due to the crystallization of ZrO<sub>2</sub> is shifted to higher temperatures compared with that for 5-FeO-ZrO<sub>2</sub> without NiSO<sub>4</sub>, indicating that there is an interaction between NiSO<sub>4</sub> and ZrO<sub>2</sub> in addition to the interaction between FeO and ZrO<sub>2</sub>. For pure NiSO<sub>4</sub>·6H<sub>2</sub>O, the DSC curve shows three endothermic peaks below 400 °C due to water elimination, indicating that the dehydration of NiSO<sub>4</sub>·6H<sub>2</sub>O occurs in three steps. The endothermic peaks in the region of 768–837 °C are due to the evolution of SO<sub>3</sub> decomposed from sulfate species.<sup>30,44</sup> Decomposition of nickel sulfate is known to begin at 700 °C.<sup>45</sup>

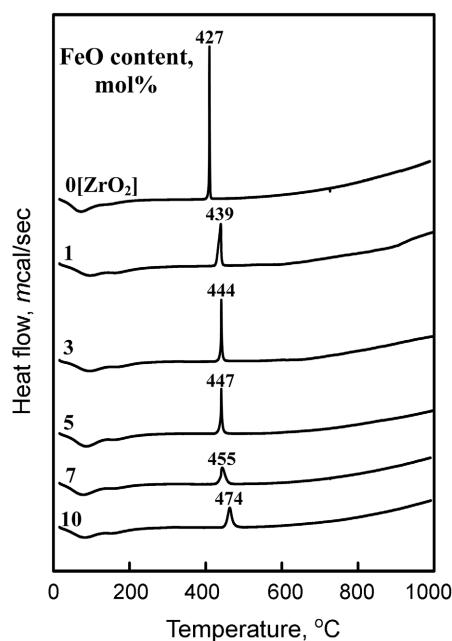


Figure 7. DSC curves of FeO-ZrO<sub>2</sub> precursors containing different FeO contents.

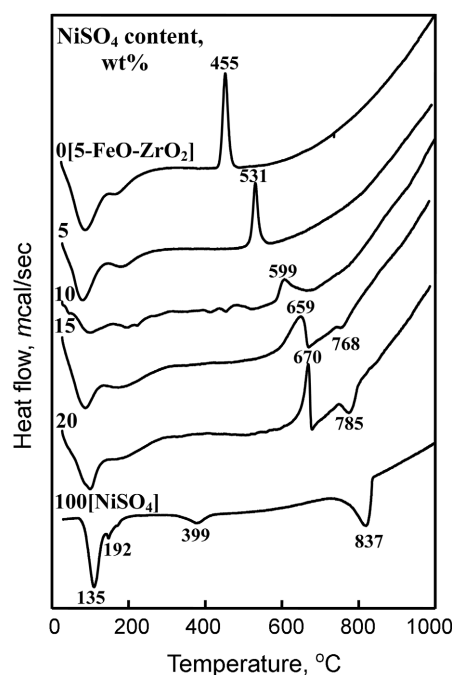


Figure 8. DSC curves of NiSO<sub>4</sub>/5-FeO-ZrO<sub>2</sub> precursors containing different NiSO<sub>4</sub> contents.

### Surface Properties.

**Specific surface area and acidity:** The specific surface areas of samples containing different NiSO<sub>4</sub> contents and calcined at 500 °C for 1.5 h are listed in Table 1. The presence of nickel sulfate and FeO influences the surface area in comparison with that of the pure ZrO<sub>2</sub>. Specific surface areas of NiSO<sub>4</sub>/5-FeO-ZrO<sub>2</sub> samples are larger than that of 5-FeO-ZrO<sub>2</sub> calcined at the same temperature, showing that surface area increases gradually with increasing

Table 1. Surface area and acidity of NiSO<sub>4</sub>/5-FeO-ZrO<sub>2</sub> catalysts containing different NiSO<sub>4</sub> contents and calcined at 500 °C for 1.5 h

NiSO <sub>4</sub> content (wt%)	Surface area (m <sup>2</sup> /g)	Acidity (μmol/g)
0	65	104
5	68	147
10	83	257
15	73	192
20	48	169

nickel sulfate loading up to 10 wt%. It seems likely that the interactions between nickel sulfate (or FeO) and ZrO<sub>2</sub> prevent catalysts from crystallizing.<sup>46</sup> The decrease of surface area for NiSO<sub>4</sub>/5-FeO-ZrO<sub>2</sub> samples containing NiSO<sub>4</sub> above 10 wt % is due to the blocking of ZrO<sub>2</sub> pores by the increased NiSO<sub>4</sub> loading. The acidity of catalysts calcined at 500 °C, as determined by the amount of NH<sub>3</sub> irreversibly adsorbed at 230 °C,<sup>20,37,38</sup> is also listed in Table 1. The variation of acidity runs parallel to the change of surface area. The acidity increases with increasing nickel sulfate content up to 10 wt % of NiSO<sub>4</sub>. The acidity is correlated with the catalytic activity for the ethylene dimerization discussed below.

**Effect of FeO addition on surface properties:** We examined the effect of FeO addition on the surface area and acidity of NiSO<sub>4</sub>/FeO-ZrO<sub>2</sub> samples. The specific surface areas and acidity of 10-NiSO<sub>4</sub>/FeO-ZrO<sub>2</sub> catalysts containing different FeO contents and calcined at 500 °C are listed in Table 2. Both surface area and acidity increased with increasing FeO content up to 5 mol%, indicating the promoting effect of FeO on the catalytic activities for ethylene dimerization discussed below.

Infrared spectroscopic studies of ammonia adsorbed on solid surfaces have made it possible to distinguish between Brønsted and Lewis acid sites.<sup>44,47,48</sup> Figure 9 shows the infrared spectra of ammonia adsorbed on 10-NiSO<sub>4</sub>/5-FeO-ZrO<sub>2</sub> samples evacuated at 500 °C for 1 h. For 10-NiSO<sub>4</sub>/5-FeO-ZrO<sub>2</sub> the band at 1453 cm<sup>-1</sup> is the characteristic peak of ammonium ion, which is formed on the Brønsted acid sites and the absorption peak at 1610 cm<sup>-1</sup> is contributed by ammonia coordinately bonded to Lewis acid sites,<sup>44,47,48</sup> indicating the presence of both Brønsted and Lewis acid sites on the surface of 10-NiSO<sub>4</sub>/5-FeO-ZrO<sub>2</sub> samples. Other samples having different nickel sulfate contents also showed

Table 2. Surface area and acidity of 10-NiSO<sub>4</sub>/FeO-ZrO<sub>2</sub> catalysts containing different FeO contents and calcined at 500 °C for 1.5 h

FeO content (mol%)	Surface area (m <sup>2</sup> /g)	Acidity (μmol/g)
0	70	121
1	72	163
3	80	208
5	83	257
7	64	168
10	61	163

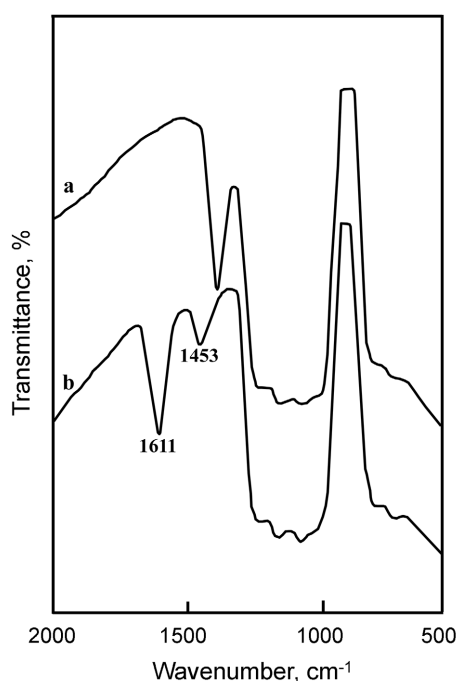


**Figure 9.** Infrared spectra of  $\text{NH}_3$  adsorbed on 10- $\text{NiSO}_4/5\text{-FeO-ZrO}_2$ : (a) background of 10- $\text{NiSO}_4/5\text{-FeO-ZrO}_2$  after evacuation at 500 °C for 1 h, (b)  $\text{NH}_3$  adsorbed on (a), where gas was evacuated at 230 °C for 1 h.

the presence of both Lewis and Brønsted acids. As Figure 9(a) shows, the intense band at 1370  $\text{cm}^{-1}$  after evacuation at 500 °C is assigned to the asymmetric stretching vibration of S=O bonds having a high double bond nature.<sup>42,44</sup> However, the drastic shift of the infrared band from 1370  $\text{cm}^{-1}$  to a lower wavenumber (not shown due to the overlaps of skeletal vibration bands of FeO-ZrO<sub>2</sub>) after ammonia adsorption [Figure 9(b)] indicates a strong interaction between an adsorbed ammonia molecule and the surface complex. Namely, the surface sulfur compound in the highly acidic catalysts has a strong tendency to reduce the bond order of S=O from a highly covalent double-bond character to a lesser double-bond character when a basic ammonia molecule is adsorbed on the catalysts.<sup>42,44</sup>

Acids stronger than  $\text{H}_0 \leq -11.93$ , which corresponds to the acid strength of 100 %  $\text{H}_2\text{SO}_4$ , are superacids.<sup>33,42,49,50</sup> The strong ability of the sulfur complex to accommodate electrons from a basic molecule such as ammonia is a driving force to generate superacidic properties.<sup>33,42,51</sup>  $\text{NiSO}_4/\text{FeO-ZrO}_2$  samples after evacuation at 500 °C for 1 h was also examined by a color change method, using Hammett indicator in sulfonyl chloride.<sup>37,52</sup> The samples were estimated to have  $\text{H}_0 \leq -14.5$ , indicating the formation of superacidic sites. Consequently,  $\text{NiSO}_4/\text{FeO-ZrO}_2$  catalysts would be solid superacids, in analogy with the case of metal oxides modified with a sulfate group.<sup>20,42,48,53</sup> This superacidic property is attributable to the double bond nature of the S=O in the complex formed by the interaction between  $\text{NiSO}_4$  and FeO-ZrO<sub>2</sub>.<sup>9,33,42,53</sup> In other words, the acid strength of  $\text{NiSO}_4/\text{FeO-ZrO}_2$  becomes stronger by the inductive effect of S=O in the complex.

### Catalytic activities for ethylene dimerization.

**Ethylene dimerization:**  $\text{NiSO}_4/\text{FeO-ZrO}_2$  catalysts were tested for their effectiveness in ethylene dimerization. Over 10- $\text{NiSO}_4/\text{ZrO}_2$ , 10- $\text{NiSO}_4/3\text{-FeO-ZrO}_2$ , and 10- $\text{NiSO}_4/5\text{-FeO-ZrO}_2$ , ethylene was continuously consumed, as shown by the results presented in Figure 10, where catalysts were evacuated at 500 °C for 1 h. Over three catalysts, ethylene was selectively dimerized to n-butenes. In the composition of n-butenes analyzed by gas chromatography, 1-butene was found to predominate exclusively at the initial reaction time, as compared with cis-butene and trans-butene. This is because the initial product of ethylene dimerization is 1-butene.<sup>4,9,48</sup> Therefore, the initially produced 1-butene is also isomerized to 2-butene during the reaction time.<sup>18-20,44</sup> As shown in Figure 10, the catalytic activities of 10- $\text{NiSO}_4/3\text{-FeO-ZrO}_2$  and 10- $\text{NiSO}_4/5\text{-FeO-ZrO}_2$  are higher than that of 10- $\text{NiSO}_4/\text{ZrO}_2$  without FeO, showing a clear FeO-promoted effect on catalytic activity for ethylene dimerization discussed below.

The catalytic activities of 10- $\text{NiSO}_4/5\text{-FeO-ZrO}_2$  were tested as a function of calcination temperature (not shown in the Figure). The activities increased with the calcination temperature, reaching a maximum at 500 °C, after which the activities decreased. The decrease of catalytic activity after calcination above 500 °C can be probably attributed to the fact that the surface area and acidity above 500 °C decrease with the calcination temperature. Thus, hereafter, emphasis is placed only on the  $\text{NiSO}_4/\text{FeO-ZrO}_2$  samples calcined at 500 °C.

**Catalytic activity as a function of  $\text{NiSO}_4$  content:** The catalytic activity of  $\text{NiSO}_4/5\text{-FeO-ZrO}_2$  containing different

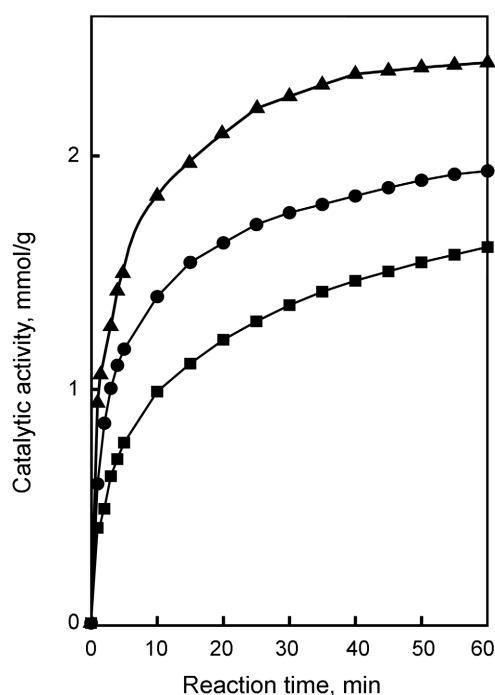


**Figure 10.** Time-course of ethylene dimerization over catalysts evacuated at 500 °C for 1 h: ( $\blacktriangle$ ), 10- $\text{NiSO}_4/5\text{-FeO-ZrO}_2$ ; ( $\bullet$ ), 10- $\text{NiSO}_4/3\text{-FeO-ZrO}_2$ ; ( $\blacksquare$ ), 10- $\text{NiSO}_4/\text{ZrO}_2$ .

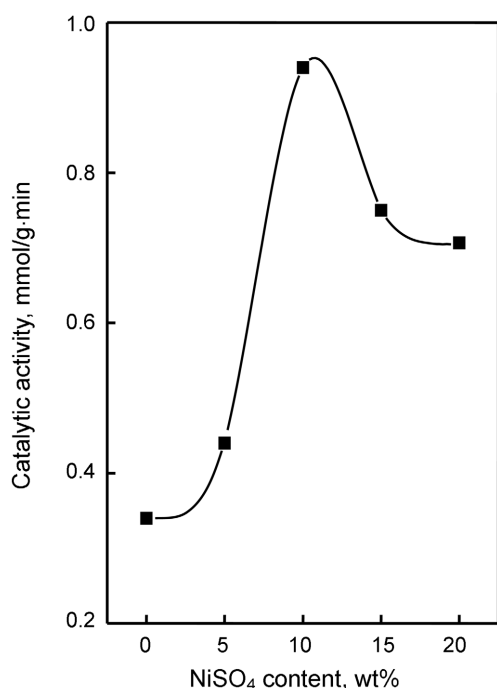


**Figure 11.** Catalytic activity of NiSO<sub>4</sub>/5-FeO-ZrO<sub>2</sub> for ethylene dimerization as a function of NiSO<sub>4</sub> content.

NiSO<sub>4</sub> contents was examined; the results are shown as a function of NiSO<sub>4</sub> content in Figure 11. Catalysts were evacuated at 500 °C for 1 h before each reaction. The catalytic activity gives a maximum at 10 wt % of NiSO<sub>4</sub>. This seems to be correlated to the specific surface area and to the acidity of catalysts. The acidity of NiSO<sub>4</sub>/5-FeO-ZrO<sub>2</sub> calcined at 500 °C was determined by the amount of NH<sub>3</sub> irreversibly adsorbed at 230 °C.<sup>20,37,38</sup> As listed in Table 1, the BET surface area attained a maximum extent when the NiSO<sub>4</sub> content in the catalyst was 10 wt % and then showed a gradual decrease with increasing NiSO<sub>4</sub> content. In view of Table 1 and Figure 11, the higher the acidity, the higher the catalytic activity. Good correlations have been found in many cases between the acidity and the catalytic activities of solid acids. For example, the rates of both the catalytic decomposition of cumene and the polymerization of propylene over SiO<sub>2</sub>-Al<sub>2</sub>O<sub>3</sub> catalysts were found to increase with increasing acid amount at strength H<sub>0</sub> ≤ +3.3.<sup>54</sup> The catalytic activity of nickel-containing catalysts in ethylene dimerization as well as in butene isomerization is closely correlated with the acidity of the catalyst.<sup>4,9,10</sup>

It is known that the active sites for ethylene dimerization consist of a low-valent nickel and an acid.<sup>4,44</sup> A low-valent nickel is favorable to chemisorb carbon monoxide and the preadsorbed CO prevents the subsequent adsorption of ethylene.<sup>44</sup> Therefore, a low-valent nickel is responsible for the adsorption site of ethylene.

**Promoting effect of FeO on catalytic activity:** The catalytic activity of 10-NiSO<sub>4</sub>/FeO-ZrO<sub>2</sub> as a function of FeO content for the reaction of ethylene dimerization was examined. Here the catalysts were evacuated at 500 °C for 1 h before reaction; the results are shown in Figure 12. The

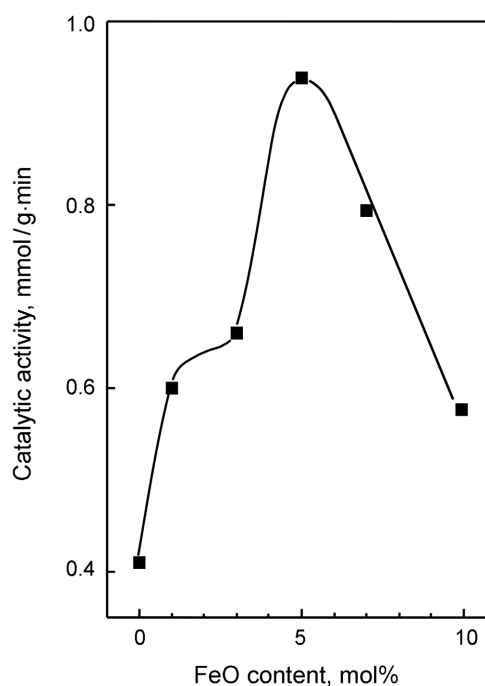


**Figure 12.** Catalytic activity of 10-NiSO<sub>4</sub>/FeO-ZrO<sub>2</sub> for ethylene dimerization as a function of FeO content.

catalytic activity increased with increasing the FeO content, reaching a maximum at 5 mol%.

Considering the experimental results of Table 2 and Figure 12, we think that the catalytic activities for ethylene dimerization are closely related to the changes of surface area and the acidity of catalysts. As listed in Table 2, the total acid sites of 10-NiSO<sub>4</sub>/5-FeO-ZrO<sub>2</sub> and 10-NiSO<sub>4</sub>/ZrO<sub>2</sub> are 257 μmol/g and 121 μmol/g, respectively, showing that the number of acid sites for the catalyst promoted with FeO is greater than that for nonpromoted catalyst. Recently, some authors reported that sulfated zirconia based mixed oxides show more stability, enhanced acidity and catalytic activity than the transition or noble metal-promoted sulfated zirconia alone.<sup>30,55,56</sup> FeO-promoted catalysts could be related to a strong interaction between FeO and ZrO<sub>2</sub>. Since the promoting effect of FeO is related to an increase in number of surface acidic sites, it would be of interest to examine various factors influencing the enhancement of these surface acidic sites.

Xia *et al.*<sup>57</sup> and Gao *et al.*<sup>58</sup> proposed that Al<sub>2</sub>O<sub>3</sub> incorporation in ZrO<sub>2</sub> matrix brought about Zr-O-Al bonds which helped to stabilize the sulfate species at the oxide surface. For the same reason, the formation of Fe-O-Zr bond on the surface of the FeO-promoted catalysts is probably the cause for the increase in strong acidic sites. At the same time, the stronger Fe-O-Zr bond formed by the charge transfer from Zr atom to neighboring Fe atom results in an increase in the thermal stability of the surface sulfate species and consequently the acidity of FeO-promoted catalyst is increased. In fact, to examine the thermal stability of the surface sulfate species DSC measurements were carried out. The endothermic peak due to the evolution of SO<sub>3</sub> decomposed from

sulfate species bonded to the surface of ZrO<sub>2</sub> appeared at 730 °C,<sup>34</sup> while that from sulfate species bonded to the surface of FeO-promoted ZrO<sub>2</sub> appeared at 768 °C. The shift of the high-temperature weight loss peak to higher temperatures for the FeO-promoted catalysts indicates an increase in the thermal stability of the surface sulfate species in these samples. Namely, the charge transfer from Zr atoms to the neighboring Fe atoms strengthens the Fe-O bond between Fe and the surface sulfate species. The stronger Fe-O bond leads to an increase in the thermal stability of the surface sulfate species and consequently the acidity of the catalysts is increased. The above results show that the incorporation of FeO is advantageous in increasing both surface area and, the acidity, which is indeed of advantage to increase the catalytic activity of the catalysts for ethylene dimerization. A similar result was related by Gao *et al.*<sup>58</sup> to strong acid sites with differential heat of ammonia adsorption above 140 kJmol<sup>-1</sup>.

### Conclusions

A series of catalysts, NiSO<sub>4</sub>/FeO-ZrO<sub>2</sub>, were prepared by the impregnation method using an aqueous solution of nickel sulfate. It is found that FeO is a good promoter for NiSO<sub>4</sub> supported on ZrO<sub>2</sub>. The addition of a small amount of FeO into NiSO<sub>4</sub>/ZrO<sub>2</sub> enhanced catalytic activity for ethylene dimerization. NiSO<sub>4</sub>/FeO-ZrO<sub>2</sub> catalysts was very effective for ethylene dimerization even at room temperature, but FeO-ZrO<sub>2</sub> without NiSO<sub>4</sub> did not exhibit any catalytic activity at all. The catalytic activity was correlated with the acidity of catalysts measured by the ammonia chemisorption method. The addition of FeO up to 5 mol % enhanced the acidity, surface area, thermal properties, and catalytic activities of NiSO<sub>4</sub>/FeO-ZrO<sub>2</sub> gradually, due to the interaction between FeO and ZrO<sub>2</sub> and due to consequent formation of Fe-O-Zr bond.

**Acknowledgements.** This work was supported by the Brain Korea 21 Project in 2003. We wish to thank Korea Basic Science Institute (Daegu Branch) for the use of their X-ray diffractometer.

### References

- Pae, Y. I.; Lee, S. H.; Sohn, J. R. *Catal. Lett.* **2005**, *99*, 241.
- Bernardi, F.; Bottoni, A.; Rossi, I. *J. Am. Chem. Soc.* **1998**, *120*, 7770.
- Sohn, J. R.; Ozaki, A. *J. Catal.* **1979**, *59*, 303.
- Sohn, J. R.; Ozaki, A. *J. Catal.* **1980**, *61*, 291.
- Wendt, G.; Fritsch, E.; Schöllner, R.; Siegel, H. *Z. Anorg. Allg. Chem.* **1980**, *467*, 51.
- Sohn, J. R.; Shin, D. C. *J. Catal.* **1996**, *160*, 314.
- Berndt, G. F.; Thomson, S. J.; Webb, G. J. *J. Chem. Soc. Faraday Trans.* **1983**, *179*, 195.
- Sohn, J. R.; Lim, J. S. *Bull. Korean Chem. Soc.* **2005**, *26*, 1029.
- Sohn, J. R.; Park, W. C.; Kim, H. W. *J. Catal.* **2002**, *209*, 69.
- Sohn, J. R.; Park, W. C. *Bull. Korean Chem. Soc.* **2000**, *21*, 1063.
- Urabe, K.; Koga, M.; Izumi, Y. *J. Chem. Soc., Chem. Commun.* **1989**, 807.
- Wendt, G.; Hentschel, D.; Finster, J.; Schöllner, R. *J. Chem. Soc. Faraday Trans.* **1983**, *179*, 2013.
- Kimura, K.; Ozaki, A. *J. Catal.* **1964**, *3*, 395.
- Maruya, K.; Ozaki, A. *Bull. Chem. Soc. Jpn.* **1973**, *46*, 351.
- Hartmann, M.; Pöpl, A.; Kevan, L. *J. Phys. Chem.* **1996**, *100*, 9906.
- Elev, I. V.; Shelimov, B. N.; Kazansky, V. B. *J. Catal.* **1984**, *89*, 470.
- Choo, H.; Kevan, L. *J. Phys. Chem. B* **2001**, *105*, 6353.
- Sohn, J. R.; Kim, H. J. *J. Catal.* **1986**, *101*, 428.
- Sohn, J. R.; Lee, S. Y. *Appl. Catal. A: Gen.* **1997**, *164*, 127.
- Sohn, J. R.; Kim, H. W.; Park, M. Y.; Park, E. H.; Kim, J. T.; Park, S. E. *Appl. Catal.* **1995**, *128*, 127.
- Hsu, C. Y.; Heimbuch, C. R.; Armes, C. T.; Gates, B. C. *J. Chem. Soc., Chem. Commun.* **1992**, 1645.
- Cheung, T. K.; Gates, B. C. *J. Catal.* **1997**, *168*, 522.
- Adeeva, V.; de Haan, H. W.; Janchen, J.; Lei, G. D.; Schunemann, V.; van de Ven, L. J. M.; Sachtler, W. M. H.; van Santen, R. A. *J. Catal.* **1995**, *151*, 364.
- Wan, K. T.; Khouw, C. B.; Davis, M. E. *J. Catal.* **1996**, *158*, 311.
- Song, X.; Reddy, K. R.; Sayari, A. *J. Catal.* **1996**, *161*, 206.
- Coelho, M. A.; Resasco, D. E.; Sikabwe, E. C.; White, R. L. *Catal. Lett.* **1995**, *32*, 253.
- Hosoi, T.; Shimadzu, T.; Ito, S.; Baba, S.; Takaoka, H.; Imai, T.; Yokoyama, N. *Prepr. Symp. Div. Petr. Chem.; American Chemical Society: Los Angeles, CA, 1988*; p 562.
- Ebitani, K.; Konishi, J.; Hattori, H. *J. Catal.* **1991**, *130*, 257.
- Signoretto, M.; Pinna, F.; Strukul, G.; Chies, P.; Cerrato, G.; Ciero, S. D.; Morterra, C. *J. Catal.* **1997**, *167*, 522.
- Hua, W.; Xia, Y.; Yue, Y.; Gao, Z. *J. Catal.* **2000**, *196*, 104.
- Moreno, J. A.; Poncelet, G. *J. Catal.* **2001**, *203*, 153.
- Sohn, J. R.; Cho, E. S. *Appl. Catal. A: Gen.* **2005**, *282*, 147.
- Tanabe, K.; Misono, M.; Ono, Y.; Hattori, H. *New Solid Acids and Bases*; Kodansha-Elsevier: Tokyo, 1989; p 185.
- Arata, K.; Hino, M.; Yamagata, N. *Bull. Chem. Soc. Jpn.* **1990**, *63*, 244.
- Sohn, J. R.; Park, E. H. *J. Ind. Eng. Chem.* **1998**, *4*, 197.
- Sohn, J. R.; Park, W. C. *Appl. Catal. A: Gen.* **2002**, *230*, 11.
- Sohn, J. R.; Cho, S. G.; Pae, Y. I.; Hayashi, S. *J. Catal.* **1996**, *159*, 170.
- Sohn, J. R.; Lee, S. H.; Park, W. C.; Kim, H. W. *Bull. Korean Chem. Soc.* **2004**, *25*, 657.
- Sohn, J. R.; Seo, D. H.; Lee, S. H. *J. Ind. Eng. Chem.* **2004**, *10*, 309.
- Sohn, J. R.; Kim, J. G.; Kwon, T. D.; Park, E. H. *Langmuir* **2002**, *18*, 1666.
- Saur, O.; Bensitel, M.; Saad, A. B. M.; Lavalley, J. C.; Tripp, C. P.; Morrow, B. A. *J. Catal.* **1986**, *99*, 104.
- Yamaguchi, T. *Appl. Catal.* **1990**, *61*, 25.
- Morrow, B. A.; McFarlane, R. A.; Lion, M.; Lavalley, J. C. *J. Catal.* **1987**, *107*, 232.
- Sohn, J. R.; Park, W. C. *Appl. Catal. A: Gen.* **2003**, *239*, 269.
- Siriwardane, R. V.; Poston, J. A.; Fisher, Jr. E. P.; Shen, M. S.; Miltz, A. L. *Appl. Surf. Sci.* **1999**, *152*, 219.
- Sohn, J. R. *J. Ind. Eng. Chem.* **2004**, *10*, 1.
- Satsuma, A.; Hattori, A.; Mizutani, K.; Furuta, A.; Miyamoto, A.; Hattori, T.; Murakami, Y. *J. Phys. Chem.* **1988**, *92*, 6052.
- Sohn, J. R.; Lee, S. H. *Appl. Catal. A: Gen.* **2004**, *266*, 89.
- Arata, K. *Adv. Catal.* **1990**, *37*, 165.
- Olah, F. G. A.; Prakash, G. K. S.; Sommer, J. *Science* **1979**, *206*, 13.
- Sohn, J. R.; Park, E. H.; Kim, H. W. *J. Ind. Eng. Chem.* **1999**, *5*, 253.
- Sohn, J. R.; Ryu, S. G. *Langmuir* **1993**, *9*, 126.
- Jin, T.; Yamaguchi, T.; Tanabe, K. *J. Phys. Chem.* **1986**, *90*, 4794.
- Tanabe, K. *Solid Acids and Bases*; Kodansha: Tokyo, 1970; p 103.
- Moreno, J. A.; Poncelet, G. *J. Catal.* **2001**, *203*, 453.
- Reddy, B. M.; Sreekanth, P. M.; Yamada, Y.; Kobayashi, T. *J. Mol. Catal. A: Chem.* **2005**, *227*, 81.
- Xia, Y.; Hua, W.; Gao, Z. *Appl. Catal. A: Gen.* **1999**, *185*, 293.
- Gao, Z.; Xia, Y.; Hua, W.; Miao, C. *Topics Catal.* **1998**, *6*, 101.